

# Modeling the Influence of Correlated Molecular Disorder on the Dynamics of Excitons in Organic Molecular Semiconductors

Chee Kong Lee,<sup>†</sup> Liang Shi,<sup>‡</sup> and Adam Willard<sup>\*,†</sup>

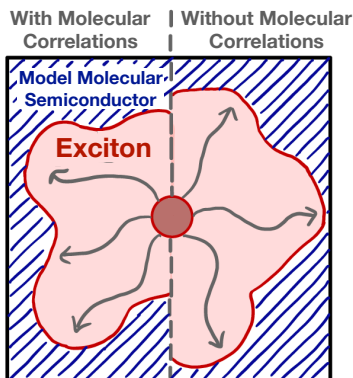
*<sup>†</sup>Department of Chemistry, Massachusetts Institute of Technology, Cambridge,  
Massachusetts 02139, USA*

*<sup>‡</sup>Chemistry and Chemical Biology, University of California, Merced, California 95343,  
United States*

E-mail: [awillard@mit.edu](mailto:awillard@mit.edu)

## Abstract

In this Letter, we investigate the role of correlated molecular disorder on the dynamics of excitons in oligothiophene-based organic semiconductors. We simulate exciton dynamics using the Frenkel exciton model and we derive parameters for this model so that they reflect the specific characteristics of all-atom molecular systems. By systematically modifying the parameters of the Frenkel exciton model we isolate the influence of spatial and temporal molecular correlations on the dynamics of excitons in these systems. We find that the molecular fluctuations inherent to these systems exhibit long-lived memory effects, but that these effects do not significantly influence the dynamic properties of excitons. We also find that excitons can be sensitive to the molecular-scale spatial correlations, and that this sensitivity grows with the amount of energetic disorder within the material. We conclude that control over spatial correlations can mitigate the negative influence of disorder on exciton transport.



The optoelectronic properties of organic molecular semiconductors are known to depend sensitively on how molecules are arranged within the material.<sup>1–8</sup> The inability to exploit this dependence for improving material performance is a problem that hinders the development of electronic applications that incorporate these materials, such as organic photovoltaic (OPV) and light-emitting (OLED) devices.<sup>9–15</sup> This problem originates, in part, from a lack of theoretical methods that can reliably predict the excited-state electronic properties of materials with disordered or irregular microscopic structure. Many efforts to address this problem have thus been focused on developing ways to accurately include the effects of disorder in traditional theoretical models.<sup>8,16–20</sup>

In this letter, we extend these efforts with a theoretical approach designed to reveal the specific effects of correlated molecular disorder on electronic energy transport in organic molecular semiconductors. Our approach combines classical molecular dynamics (MD) simulations, semiempirical electronic structure calculations, and the Frenkel exciton model, in order to identify the characteristics of molecular correlations in these materials and isolate their influence on the microscopic dynamics of electronic excitations. Using this approach, we find that energy transport in these materials can be very sensitive to the presence of spatial correlations, and that this sensitivity depends on the width of the distribution of excitation energies. We illustrate that fluctuations in these energies play a fundamental role in driving the dynamics of electronic excitations, but we also highlight that these dynamics are insensitive to the temporal correlations that arise due to regular nuclear vibrations.

These findings suggest that it may be necessary to consider the interplay between correlated and uncorrelated disorder when applying molecular design principles to the development of organic molecular semiconductors.

Energy transport in organic conjugated systems is determined primarily by the microscopic dynamics of Coulombically bound excited electron-hole pairs, known as excitons. In condensed phase systems, intermolecular electronic coupling can drive excitons to delocalize across many individual molecules. The properties of these delocalized excitons depend on the strengths of electronic couplings and on how they are distributed in space and time. The characteristics of a material’s molecular structure that are most relevant to the dynamics of excitons are thus encoded in these electronic coupling distributions. Unfortunately, these distributions are difficult to compute because they require evaluation of the excited state electronic structure and because they tend to vary significantly with small changes in nuclear configuration and therefore must be computed separately for each pair of molecules in the system.

The computation of electronic properties is not the only challenge associated with modeling exciton dynamics in disordered systems. Accurate modeling also requires the ability to address system sizes large enough to fully accommodate delocalized excitons, and a sampling scheme capable of capturing the effects that arise due to local variations in molecular structure. If excitons delocalize over more than a few molecules, then standard electronic structure methods, such as those based on density functional theory, are generally too computationally expensive to fully meet these requirements. As an alternative, site-based phenomenological models provide a simple and efficient platform for computing the static and dynamic properties of delocalized excitons in extended heterogeneous systems.

Here, we simulate the properties of delocalized excitons using the Frenkel exciton model<sup>21,22</sup> in which the excited electronic properties of a N-molecule system are expressed in terms of

the Frenkel Hamiltonian,

$$H(t) = \sum_i \epsilon_i(t) |i\rangle \langle i| + \sum_{ij} V_{ij}(t) |i\rangle \langle j|, \quad (1)$$

where  $|i\rangle$  represents a state with an exciton localized on molecule  $i$ ,  $\epsilon_i$  denotes the energy of that state, and  $V_{ij}$  denotes the intermolecular electronic coupling between states  $|i\rangle$  and  $|j\rangle$ . Because this simple model lacks explicit chemical detail, all aspects of a system’s molecular structure must be described implicitly, in terms of model parameters. For this reason, the effects of molecular disorder are often incorporated into this model by dressing static model parameters with additional random components. The characteristics of these random components are often assumed to be Gaussian distributed, spatially uncorrelated, and described by simple dynamics that are either temporally uncorrelated (e.g., white noise) or arising from weak coupling to a bath of harmonic oscillators.<sup>18,23–26</sup> Although these assumptions introduce disorder in a well defined and easily controllable manner, it is not obvious to what extent the molecular structure that they imply is physically realistic.

In our approach, the parameters of the Frenkel Hamiltonian are assigned non-randomly based on the microscopic structure of configurations generated with all-atom MD simulation (see supplementary information for more details). We consider the effect of thermal fluctuations on the statistics of these model parameters, and we quantify the spatial and temporal correlations that are associated with these statistics. By determining the separate influences of these correlations on the dynamics of excitons we can critically assess the assumptions that are commonly applied when parameterizing the Frenkel exciton model for organic molecular semiconductors. We present results for room temperature ( $T = 300\text{K}$ ) condensed phase systems that are made up entirely of assembled sexithiophene (T6) molecules. We choose T6-based materials specifically because they have been well studied both experimentally and theoretically.<sup>27–30</sup> We consider systems with two different characteristic morphologies: a monolayer film of 150 longitudinally aligned molecules and an amorphous bulk of 343 T6

molecules. These systems are illustrated in Fig. 1(a).

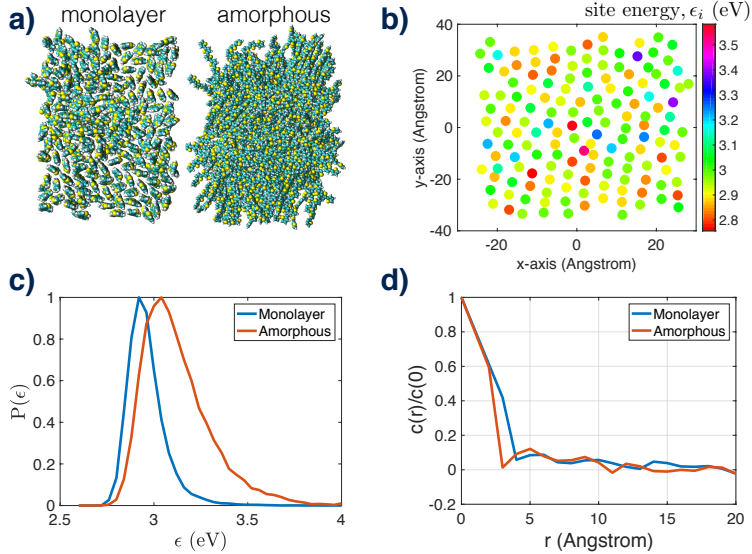


Figure 1: (a) Snapshots from MD simulations of the disordered monolayer film of T6 molecules (left) and the amorphous aggregate of T6 molecules (right). (b) A plot illustrating the spatial energetic disorder derived from a single configuration of the disordered monolayer film. Point positions represent the lateral center of mass of each molecule in the system and shading represents the molecular excitation energy, *i.e.*, the site energy  $\epsilon_i$ , derived from our method. (c) The probability distributions of site energies as sampled from 100 MD configurations of the monolayer film (blue) and the amorphous aggregate (red). (d) The spatial correlation function for site energies of molecules with center of mass separation  $r$ , averaged over configurations of the monolayer film (blue) and amorphous aggregate (red).

In Fig. 1 we illustrate how differences in molecular structure influence the characteristics of site energetic disorder. Fig. 1(b) shows the spatial distribution of site energies (*i.e.*,  $\epsilon_i$  in Eq. 1) as derived by applying our parameterization method to a single MD configuration of the monolayer film. This plot illustrates that the monolayer film includes significant spatial disorder, because the molecules are not arranged on a regular lattice, and significant energetic disorder, because molecules exhibit a wide range of excitation energies.

Fig. 1(c) contains a plot of  $P(\epsilon)$ , the probability for a molecule in a given system to have a site energy  $\epsilon$ . We observe that  $P(\epsilon)$  is broad and asymmetric for both the monolayer and the amorphous system, which have a standard deviations of 0.10eV and 0.18eV, respectively. The distribution of the monolayer system is both red-shifted and narrowed

relative to that of the amorphous system. These differences reflect the influence of favorable  $\pi$ -stacking interactions between neighboring molecules in the film, which simultaneously limit configurational variations and promotes conjugation through molecular planarization.

Molecular packing effects in condensed phase systems can lead to the emergence of spatial correlations in molecular and electronic structure. These correlations are often neglected when assigning parameters in the Frenkel exciton model. Our approach to assigning these parameters preserves these correlations, which enables them to be quantified. We define the spatial correlation function for site energies as,

$$c(r) = \langle (\epsilon_i - \bar{\epsilon})(\epsilon_j - \bar{\epsilon})\delta(r_{ij} - r) \rangle \quad (2)$$

where  $\langle \cdot \cdot \cdot \rangle$  denotes an average over all available configurations of a given system,  $\bar{\epsilon}$  is the average site energy for molecules in the system,  $r_{ij}$  is the center-of-mass separation between the molecules associated with sites  $i$  and  $j$ , and  $\delta(x)$  is the Dirac delta function.

Fig. 1(d) contains a plot of  $c(r)$  for the monolayer film and the amorphous bulk systems. As this plot illustrates, closely spaced molecules tend to have correlated excitation energies. We observe that these correlations die off rapidly with distance, not extending much beyond distances of about 0.5nm (i.e., roughly the nearest neighbor distance), but are slightly longer ranged in the monolayer system. Despite the lack of long-range spatial correlations, it has been found that excitons readily delocalize in both of these systems.<sup>20</sup>

The time dependence of the model parameters in Eq. 1 are generated to reflect the evolution of a given system from MD simulation. A representative trace of  $\epsilon(t)$  for a single site of the model monolayer film, as plotted in the inset of Fig. 2(a), reveals that the excitation energy of individual molecules can exhibit significant fluctuations. The temporal correlations in these model parameters can be characterized by computing the time correlation function for site energies,

$$C_\epsilon(t) = \frac{\langle (\epsilon_i(t) - \bar{\epsilon}_i)(\epsilon_i(0) - \bar{\epsilon}_i) \rangle}{\langle (\epsilon_i(0) - \bar{\epsilon}_i)^2 \rangle}, \quad (3)$$

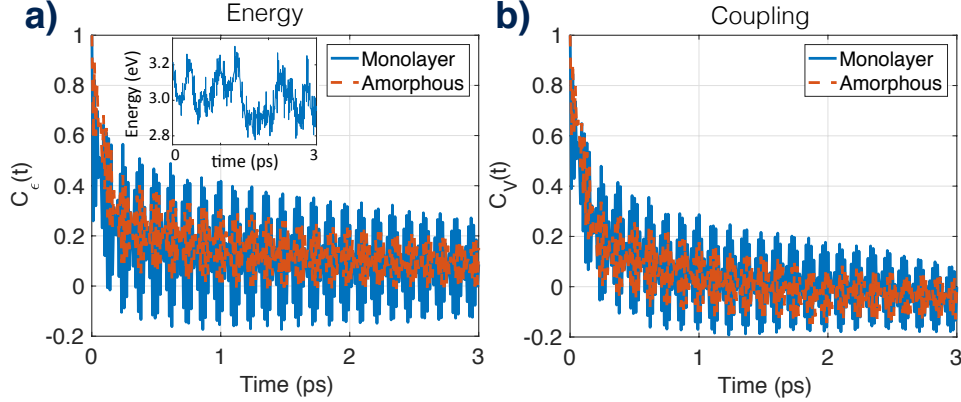


Figure 2: (a) The time correlation function for state energies in the monolayer film (solid blue) and the amorphous aggregate (dashed red). Inset shows the fluctuations in  $\epsilon_i$  computed a long a single trajectory of the monolayer film for a single site. (b) The time correlation for intermolecular couplings, averaged over all possible molecular pairs, in the monolayer film (solid blue) and the amorphous system (dashed red).

and for intermolecular electronic couplings,

$$C_V(t) = \frac{\langle (V_{ij}(t) - \bar{V}_{ij})(V_{ij}(0) - \bar{V}_{ij}) \rangle}{\langle (V_{ij}(0) - \bar{V}_{ij})^2 \rangle}, \quad (4)$$

where the averages implied by  $\langle \dots \rangle$  include data generated for a system with a given molecular structure and the overbars indicate time average. As illustrated in Fig. 2, both  $C_\epsilon(t)$  and  $C_V(t)$  exhibit non-trivial forms, including distinct short and long time decay profiles along with a remarkably long lived oscillatory feature. For both correlation functions we attribute the initial fast decay (*i.e.*,  $\tau \sim 100$ fs) to the dephasing effect from nuclear ballistic motion, and the slower decay (*i.e.*,  $\tau \sim 500$ fs) to ring-ring torsional dynamics. We attribute the long lived oscillations, with periods of approximately 20fs and 100fs, to the C-H and C-C bond stretching vibrations, respectively. These correlations are significantly more complicated than what is usually assumed in applications of the Frenkel model to organic molecular semiconductors.<sup>18,23,24,26</sup> Some previous efforts to develop more realistic descriptions of the phonon spectral density have combined MD simulation with excited state electronic structure calculation,<sup>31-34</sup> however, due to computational cost these efforts have been limited to relatively small system sizes and short time scales.

To investigate how the molecular correlations in these materials influence the dynamics of excitons we carry out simulations using the time-dependent Hamiltonian in Eq. 1. Specifically, we solve the time-dependent Schrodinger equation to obtain the exciton wavefunction,

$$|\psi(t)\rangle = \hat{T}e^{-\frac{i}{\hbar} \int H(t')dt'} |\psi(0)\rangle = \sum_i c_i(t) |i\rangle, \quad (5)$$

where  $\hat{T}$  is the time-ordering operator and  $c_i(t)$  is the wavefunction coefficient in the molecular site basis. We then isolate the influence of specific correlations by modifying the Hamiltonian, replacing correlated parameters with uncorrelated random noise. By using the time dependent Frenkel Hamiltonian derived from MD simulations we are able to capture the effect of nuclear motion on the properties of the exciton, however, this approach to dynamics omits the feedback of the exciton on the dynamics of the nuclei. Omitting this feedback yields a significant gain in computational efficiency, however, the resulting electronic dynamics are thus prevented from properly thermalizing. Since the transient effects associated with exciton thermalization are most pronounced on timescales that are longer than we simulate here,<sup>35,36</sup> we expect the errors associated with the omission of this feedback to be small and have no influence on the nature of our conclusions. This issue is discussed more thoroughly in the Supporting Information.

We quantify the dynamic properties of excitons in terms of their mean-squared displacements (MSD), which we compute from the solution to Eq. 5 using the formula,

$$MSD(t) = \langle \sum_i |c_i(t)|^2 \mathbf{r}_i^2(t) \rangle, \quad (6)$$

where  $\mathbf{r}_i$  denotes the center-of-mass position of the molecule associated with site  $i$ . We compute the MSD by averaging over a nonequilibrium ensemble of trajectories that are each initialized with the exciton localized on a single site. Similarly, the delocalization of excitons can be quantified in terms of the inverse participation ratio, as presented in the Supporting Information.

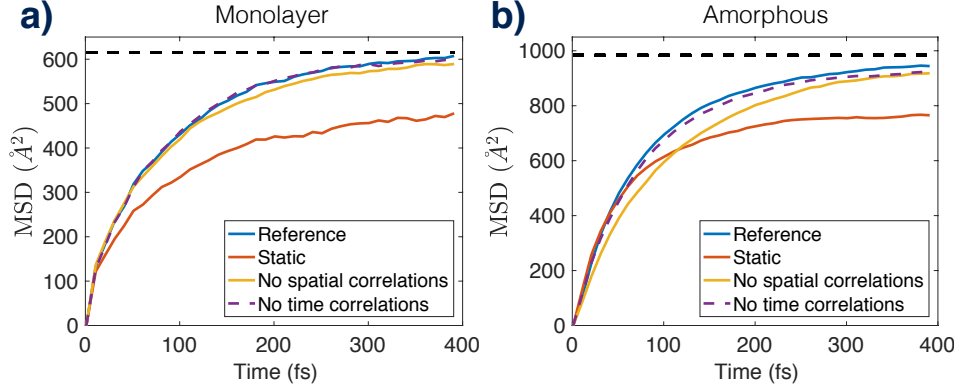


Figure 3: The MSD of an initially localized exciton in (a) the monolayer film and (b) amorphous bulk under different model conditions. In both panels the fully mapped reference condition is represented with a solid blue line, the static condition is represented with a solid red line, the condition with no spatial correlations is represented by a solid yellow line, and the condition with no temporal correlations is represented by a dashed magenta line. The black dashed lines denote MSD between a localized and fully delocalized exciton.

We compare the exciton dynamics generated under four different sets of model conditions. The first condition is the reference condition, in which the parameters of  $H(t)$  are mapped directly from the results of MD simulations following the method in Ref. 20. The second condition is a static condition, designed to evaluate the effect of molecular fluctuations on the dynamics of excitons. For the static condition all model parameters are time independent, mapped from a single randomly drawn configuration from the MD simulations. The third and fourth set of model conditions modify those of the reference condition by eliminating either spatial or temporal correlations in the model parameters, respectively.

Under the third set of model conditions, spatial correlations are eliminated by assigning  $\epsilon_i(0)$  for each site randomly from the distributions in Fig. 1(c), but the time-dependent component  $\delta\epsilon_i(t) = \epsilon_i(t) - \epsilon_i(0)$  for each site remains identical to that of the fully mapped reference Hamiltonian. With this set of conditions  $V_{ij}(t)$  is left unmodified from the reference Hamiltonian. Under the fourth set of model conditions, temporal correlations are eliminated from the time-dependent components  $\delta\epsilon_i(t)$  and  $\delta V_{ij}(t) = V_{ij}(t) - V_{ij}(0)$  by assigning both as Gaussian white noise with the same variance as the reference Hamiltonian.

The MSD computed for each of the four conditions are plotted in Fig. 3. We find

that under the reference condition, excitons in both the monolayer and the amorphous systems exhibit similar dynamics, with  $\sim 100$ fs of rapid diffusion followed by a plateauing as excitons reach the system boundaries. We observe that for the static conditions the initial exciton dynamics are similar but they taper off early (*i.e.*,  $t \geq 50$ fs) due to the onset of Andersen localization.<sup>37</sup> These results thus indicate that while molecular fluctuations are central to sustaining the excitons dynamics in these systems, their local mobility is primarily determined by the distribution of electronic couplings.

Fig. 3 also illustrates that exciton dynamics in these materials are not sensitive to the non-Markovian time correlations exhibited by  $C_\epsilon(t)$  and  $C_V(t)$  in Fig. 2. Specifically, the model conditions without time correlations reveal that the MSD for excitons is essentially unaffected when the dynamics of the fully mapped reference Hamiltonian are replaced with Gaussian white noise. Notably, these results are consistent with a similar finding that non-Markovian effect in biological light harvesting systems do not play a significant role in the exciton dynamics at room temperature.<sup>38</sup> To expand upon this point, we compare the statistics of exciton displacements across many individual trajectories. In Fig. 4 we plot the probability distribution,  $P(D^2)$ , where  $D^2 = \sum_i |c_i(t)|^2 \mathbf{r}_i^2(t)$  is the squared displacement of an exciton computed from a single trajectory. This figure illustrates that the statistics of exciton displacements are similar for both systems under model conditions with or without time correlations.

The MSD for excitons generated under model conditions without spatial correlations, as plotted in Fig. 3, reveals that the influence of spatial correlations on exciton dynamics is system dependent. Removing spatial variations from the reference model has minimal effect in the monolayer film, however, in the amorphous system the absence of spatial correlations results in a reduction of exciton diffusivity. Because the spatial correlations for each system are very similar (see Fig. 1(d)), the origin of this system dependence must involve a different aspect of molecular structure.

Based on the difference in  $P(\epsilon)$  between the two systems (*e.g.*, Fig. 1)c, we hypothesize

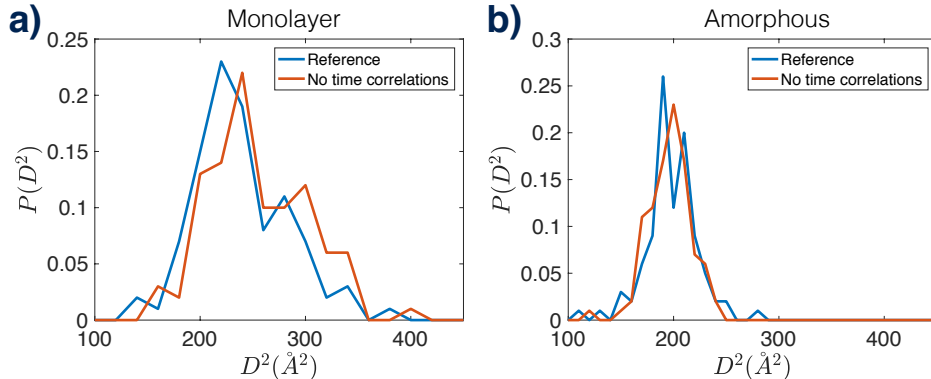


Figure 4: Probability distributions of exciton displacements computed from individual trajectories  $t = 100\text{fs}$  after being initialized on a single site. Each distribution is calculated from 100 independent trajectories of the (a) monolayer film and (b) amorphous bulk systems. In each panel the blue line indicates the fully-mapped reference model condition and the red line indicates the model conditions with no time correlations.

that the sensitivity of exciton dynamics to spatial correlations is mediated by the amplitude of energetic disorder in the system. We test this hypothesis by artificially amplifying the disorder in the  $\epsilon_i$ 's in the model amorphous film with and without the inclusion of spatial correlations. As illustrated in Fig. 5, if the amplitude of disorder in this system is systematically increased, then the overall exciton diffusivity decreases (as expected) and the difference between the MSDs with and without spatial correlations grows. In other words, the effect of spatial correlations on exciton dynamics grows more pronounced as the microscopic structure of a system is made more disordered.

As Fig. 5 summarizes, the importance of spatial correlations on exciton dynamics depends on the amount of energetic disorder in the system. This observation implies that current rule-of-thumb design criteria may be insufficient for guiding ongoing material development efforts. In addition, this implies that control over spatial correlations can possibly mitigate the negative influence of disorder on exciton transport properties. We have also found that exciton dynamics in these systems are insensitive to the details of temporal correlations, however, this insensitivity may not necessarily persist in all organic molecular semiconductors. Simple phenomenological models, such as we have utilized here, provide a convenient and efficient framework for exploring the interplay between molecular structure and opto-

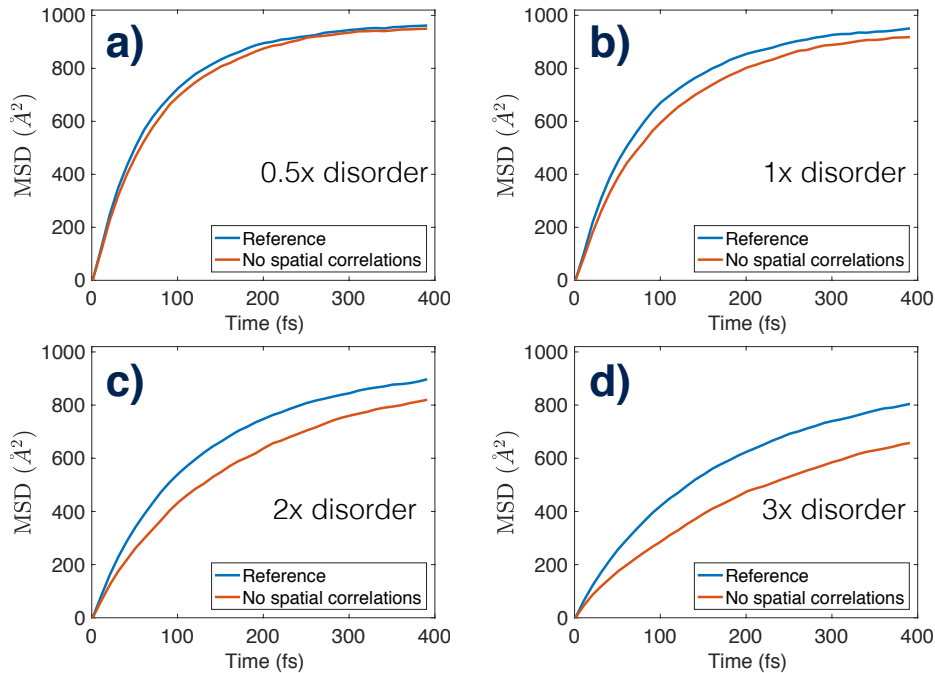


Figure 5: MSD of an initially localized exciton in amorphous bulk system generated from full molecular calculations, but with the magnitude of static energetic disorder artificially amplified by a factor of (a) 0.5, (c) 2 or (d) 3. For comparison, panel (b) contains the unamplified distribution.

electronic material properties. The continued development and application of these modeling approaches is thus important for advancing our understanding of these systems.

*Acknowledgements* – This work was supported by the Center for Excitonics, an Energy Frontier Research Center funded by the U.S. Department of Energy, Office of Science, Office of Basic Energy Sciences under Award No. DE-SC0001088 and by the Research Corporation for Scientific Advancement through a Cottrell Scholars Award. This research used resources of the National Energy Research Scientific Computing Center (NERSC), a U.S. Department of Energy Office of Science User Facility operated under Contract No. DE-AC02-05CH11231.

## References

- (1) Clark, J.; Silva, C.; Friend, R. H.; Spano, F. C. Role of intermolecular coupling in the photophysics of disordered organic semiconductors: aggregate emission in regioregular

- polythiophene. *Phys. Rev. Lett.* **2007**, *98*, 206406.
- (2) Thorsmølle, V. K.; Averitt, R. D.; Demsar, J.; Smith, D.; Tretiak, S.; Martin, R.; Chi, X.; Crone, B.; Ramirez, A.; Taylor, A. Morphology effectively controls singlet-triplet exciton relaxation and charge transport in organic semiconductors. *Phys. Rev. Lett.* **2009**, *102*, 017401.
- (3) Hiszpanski, A. M.; Baur, R. M.; Kim, B.; Tremblay, N. J.; Nuckolls, C.; Woll, A. R.; Loo, Y.-L. Tuning polymorphism and orientation in organic semiconductor thin films via post-deposition processing. *J. Am. Chem. Soc.* **2014**, *136*, 15749–15756.
- (4) Huang, Y.; Kramer, E. J.; Heeger, A. J.; Bazan, G. C. Bulk heterojunction solar cells: morphology and performance relationships. *Chem. Rev.* **2014**, *114*, 7006–7043.
- (5) Pfattner, R.; Bromley, S. T.; Rovira, C.; Mas-Torrent, M. Tuning crystal ordering, electronic structure, and morphology in organic semiconductors: Tetrathiafulvalenes as a model case. *Adv. Funct. Mater.* **2016**, *26*, 2256–2275.
- (6) Riera-Galindo, S.; Tamayo, A.; Mas-Torrent, M. Role of Polymorphism and Thin-Film Morphology in Organic Semiconductors Processed by Solution Shearing. *ACS Omega* **2018**, *3*, 2329–2339.
- (7) Hu, Z.; Adachi, T.; Haws, R.; Shuang, B.; Ono, R. J.; Bielawski, C. W.; Landes, C. F.; Rossky, P. J.; Vanden Bout, D. A. Excitonic energy migration in conjugated polymers: The critical role of interchain morphology. *J. Am. Chem. Soc.* **2014**, *136*, 16023–16031.
- (8) Tapping, P. C.; Clifton, S. N.; Schwarz, K. N.; Kee, T. W.; Huang, D. M. Molecular-level details of morphology-dependent exciton migration in poly (3-hexylthiophene) nanostructures. *J. Phys. Chem. C* **2015**, *119*, 7047–7059.
- (9) Burroughes, J.; Bradley, D.; Brown, A.; Marks, R.; Mackay, K.; Friend, R.; Burns, P.;

- Holmes, A. Light-emitting diodes based on conjugated polymers. *Nature* **1990**, *347*, 539.
- (10) Friend, R.; Gymer, R.; Holmes, A.; Burroughes, J.; Marks, R.; Taliani, C.; Bradley, D.; Dos Santos, D.; Bredas, J.; Lögdlund, M.; Salaneck, W. Electroluminescence in conjugated polymers. *Nature* **1999**, *397*, 121.
- (11) Hains, A. W.; Liang, Z.; Woodhouse, M. A.; Gregg, B. A. Molecular semiconductors in organic photovoltaic cells. *Chem. Rev.* **2010**, *110*, 6689–6735.
- (12) Mishra, A.; Bäuerle, P. Small molecule organic semiconductors on the move: promises for future solar energy technology. *Angew. Chem.* **2012**, *51*, 2020–2067.
- (13) Köhler, A.; Bässler, H. *Electronic processes in organic semiconductors: An introduction*; John Wiley & Sons, 2015.
- (14) Ostroverkhova, O. Organic optoelectronic materials: mechanisms and applications. *Chem. Rev.* **2016**, *116*, 13279–13412.
- (15) Kalyani, N. T.; Dhoble, S. Organic light emitting diodes: Energy saving lighting technology – A review. *Renewable and Sustainable Energy Reviews* **2012**, *16*, 2696–2723.
- (16) Gierschner, J.; Huang, Y.-S.; Van Averbeke, B.; Cornil, J.; Friend, R. H.; Beljonne, D. Excitonic versus electronic couplings in molecular assemblies: The importance of non-nearest neighbor interactions. *J. Chem. Phys.* **2009**, *130*, 044105.
- (17) Cheung, D. L.; Troisi, A. Theoretical study of the organic photovoltaic electron acceptor PCBM: Morphology, electronic structure, and charge localization. *J. Phys. Chem. C* **2010**, *114*, 20479–20488.
- (18) Lee, C. K.; Moix, J.; Cao, J. Coherent quantum transport in disordered systems: A unified polaron treatment of hopping and band-like transport. *J. Chem. Phys.* **2015**, *142*, 164103.

- (19) Aragó, J.; Troisi, A. Regimes of exciton transport in molecular crystals in the presence of dynamic disorder. *Adv. Funct. Mater.* **2016**, *26*, 2316–2325.
- (20) Shi, L.; Willard, A. P. Modeling the effects of molecular disorder on the properties of Frenkel excitons in organic molecular semiconductors. *J. Chem. Phys.* **2018**, *149*, 094110.
- (21) Frenkel, J. On the transformation of light into heat in solids. I. *Phys. Rev.* **1931**, *37*, 17.
- (22) Davydov, A. S. The theory of molecular excitons. *Physics-Uspeski* **1964**, *7*, 145–178.
- (23) Haken, H.; Reineker, P. The coupled coherent and incoherent motion of excitons and its influence on the line shape of optical absorption. *Zeitschrift für Physik* **1972**, *249*, 253–268.
- (24) Haken, H.; Strobl, G. An exactly solvable model for coherent and incoherent exciton motion. *Zeitschrift für Physik* **1973**, *262*, 135–148.
- (25) Rebentrost, P.; Chakraborty, R.; Aspuru-Guzik, A. Non-Markovian quantum jumps in excitonic energy transfer. *J. Chem. Phys.* **2009**, *131*, 11B605.
- (26) Moix, J. M.; Khasin, M.; Cao, J. Coherent quantum transport in disordered systems: I. The influence of dephasing on the transport properties and absorption spectra on one-dimensional systems. *New J. Phys.* **2013**, *15*, 085010.
- (27) Oelkrug, D.; Egelhaaf, H.-J.; Haiber, J. Electronic spectra of self-organized oligothiophene films with “standing” and “lying” molecular units. *Thin Solid Films* **1996**, *284*, 267–270.
- (28) Fichou, D. *Handbook of oligo-and polythiophenes*; John Wiley & Sons, 2008.
- (29) Perepichka, I. F.; Perepichka, D. F. *Handbook of Thiophene-Based Materials: Applications in Organic Electronics and Photonics, 2 Volume Set*; John Wiley & Sons, 2009.

- (30) Varene, E.; Bogner, L.; Bronner, C.; Tegeder, P. Ultrafast exciton population, relaxation, and decay dynamics in thin oligothiophene films. *Phys. Rev. Lett.* **2012**, *109*, 207601.
- (31) Aghtar, M.; Strümpfer, J.; Olbrich, C.; Schulten, K.; Kleinekathöfer, U. The FMO complex in a glycerol–water mixture. *J. Phys. Chem. B* **2013**, *117*, 7157–7163.
- (32) Valleau, S.; Eisfeld, A.; Aspuru-Guzik, A. On the alternatives for bath correlators and spectral densities from mixed quantum-classical simulations. *J. Chem. Phys.* **2012**, *137*, 224103.
- (33) Olbrich, C.; Strümpfer, J.; Schulten, K.; Kleinekathöfer, U. Theory and simulation of the environmental effects on FMO electronic transitions. *J. Phys. Chem. Lett.* **2011**, *2*, 1771–1776.
- (34) Shim, S.; Rebentrost, P.; Valleau, S.; Aspuru-Guzik, A. Atomistic study of the long-lived quantum coherences in the Fenna-Matthews-Olson complex. *Biophys. J.* **2012**, *102*, 649–660.
- (35) Lee, E. M.; Tisdale, W. A.; Willard, A. P. Perspective: Nonequilibrium dynamics of localized and delocalized excitons in colloidal quantum dot solids. *Journal of Vacuum Science & Technology A: Vacuum, Surfaces, and Films* **2018**, *36*, 068501.
- (36) Azzaro, M. S.; Dodin, A.; Zhang, D. Y.; Willard, A. P.; Roberts, S. T. Exciton-Delocalizing Ligands Can Speed Up Energy Migration in Nanocrystal Solids. *Nano letters* **2018**, *18*, 3259–3270.
- (37) Anderson, P. W. Absence of Diffusion in Certain Random Lattices. *Phys. Rev.* **1958**, *109*, 1492–1505.
- (38) Jang, S.; Hoyer, S.; Fleming, G.; Whaley, K. B. Generalized master equation with non-

markovian multichromophoric förster resonance energy transfer for modular exciton densities. *Phys. Rev. Lett.* **2014**, *113*, 188102.

## Supporting Information

### 1. Inverse Participation Ratio

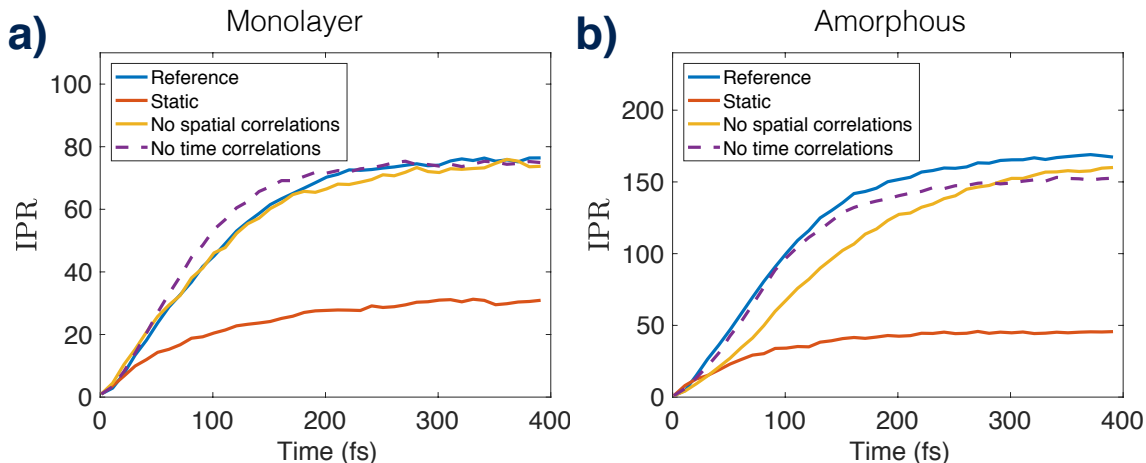


FIG. 1: The average IPR of an initially localized exciton in (a) monolayer film and (b) amorphous bulk under different model conditions. In both panels the fully mapped reference condition is represented with a solid blue line, the static condition is represented with a solid red line, the condition with no spatial correlations is represented by a solid yellow line, and the condition with no temporal correlations is represented by a dashed magenta line.

A useful measure to characterize the extent of delocalization of exciton wavefunction is the inverse participation ratio (IPR) [1]

$$\text{IPR} = \sum_i \frac{1}{|c_i(t)|^4}, \quad (1)$$

where  $c_i(t)$  is the wavefunction coefficient in the site basis from the solution of the time-dependent Schrodinger equation. IPR represents qualitatively the number of sites/molecules “participates” in the wavefunction and serve as an alternative measure of exciton transport to mean-squared-displacement (MSD). For example, if the exciton wavefunction is localized in just one molecule, the then  $\text{IPR} = 1$ . On the other hand, if exciton wavefunction is evenly delocalized in a system of  $N$  sites/molecules,  $\text{IPR} = N$  since  $c_i = 1/\sqrt{N}$ . IPRs generated from the fully mapped reference Hamiltonian in Eq. 1 in the main text for monolayer film and the amorphous bulk with initially localized exciton are plotted in Fig. 1 (solid blue lines). In both systems, IPRs increase rapidly within the first 200fs before plateauing due

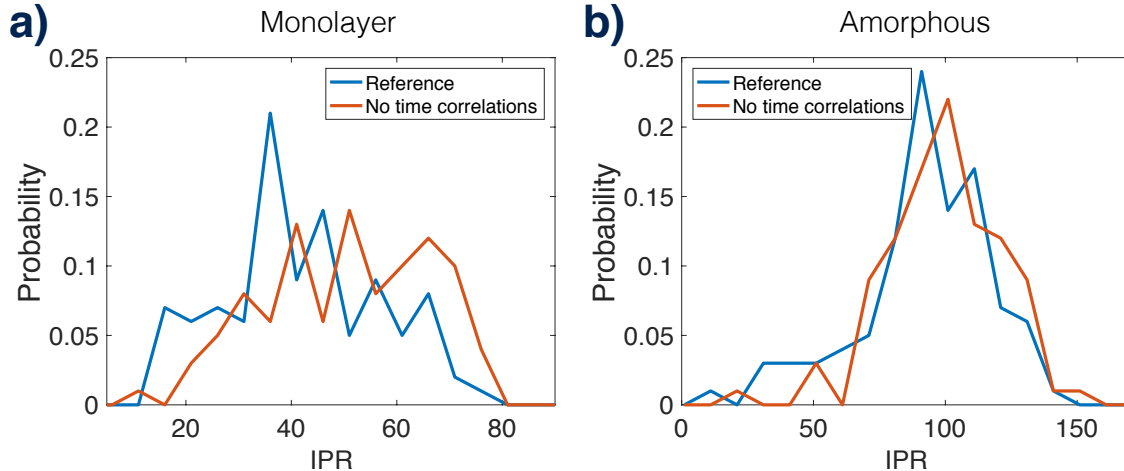


FIG. 2: Probability distributions of exciton displacements computed from individual trajectories  $t = 100\text{fs}$  after being initialized on a single site. Each distribution is calculated from 100 independent trajectories of the (a) monolayer film and (b) amorphous bulk systems. In each panel the blue line indicates the fully-mapped reference model condition and the red line indicates the model conditions with no time correlations.

to the finite-size effect. The final value of IPR for the amorphous bulk is higher because of its larger system size compared to the monolayer film.

We also explore IPRs generated under three other different conditions in Fig. 1: calculations with static Hamiltonian (solid red lines), calculations with no spatial correlation in the static disorder (solid orange lines), and calculations with no time correlation in the time-dependent fluctuations (dashed magenta lines). In general, the qualitative behaviors under each condition are very similar to those found in the analysis of MSDs in the main text. IPRs generated from the same Hamiltonian but without the time-dependent components (i.e.  $\delta V_{ij}(t) = 0$  and  $\delta \epsilon_i(t) = 0$ ) results in a significantly reduced IPR due to the Anderson localization effect. Fig. 1 also shows that temporal correlation does not play an important role in exciton transport as the IPR generated from the Hamiltonian without temporal correlation (dashed magenta lines) is nearly identical to the IPR generated from the molecular simulations (solid blue lines). The distributions of IPRs at  $t = 100\text{fs}$  sampled from 100 initial configurations are plotted in FIG. 2, which again shows that the IPR distributions generated from molecular simulations and from Hamiltonian with white noise to be similar, confirming the minimal effect of temporal correlation. Similar to the findings in the main

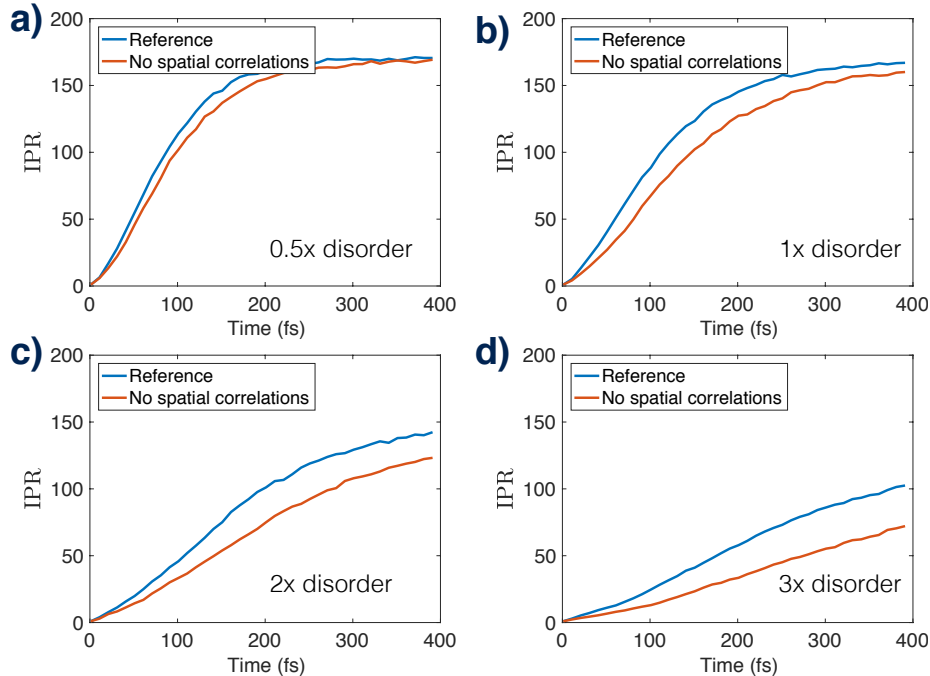


FIG. 3: IPR of an initially localized exciton in disordered film generated from full molecular calculations, but with the magnitude of static energetic disorder artificially amplified by a factor of (a) 0.5, (c) 2 or (d) 3. For comparison, panel (b) contains the unamplified distribution.

text, the effect of spatial correlation on IPRs is system dependent: it has little effect on the monolayer film, but reduces the IPR in the disordered film (dashed lines in FIG. 1). FIG. 3 shows the IPR in disordered film with its static disorder artificially increased, and our results demonstrate that the effect of spatial correlation on IPR increases with the magnitude of static disorder.

## 2. Parametrization of Frenkel Hamiltonian

We follow a recently developed method for mapping the structure of a  $N$ -molecule configuration onto the parameters of a corresponding  $N \times N$  Frenkel Hamiltonian matrix. In this method, molecular configurations are generated using classical molecular dynamics (MD) simulations and each individual configuration is translated into Frenkel model parameters based on the analysis of  $N$  single-molecule excited state electronic structure calculations. Specifically, for a given configuration we perform a single electronic structure calculation

on each individual molecule, treating all other molecules as an effective dielectric medium. Electronic structure is computed using a semiempirical Pariser-Parr-Pople (PPP) Hamiltonian with excited state properties computed at the level of configuration interactions singles. Intermolecular couplings are evaluated by computing the diabatic coupling between the locally excited molecule pairs through transition densities. A complete description of this method, including information about classical force fields, electronic structure methods, and benchmarking against higher level theories can be found in Ref. [2].

### 3. Exciton Dynamics Without Excited State Forces

We have chosen to simulate exciton dynamics with a method that omits the effects of excited state nuclear forces. In our method, the dynamics of the classical subsystem evolve on the potential energy surface of the electronic ground state, and are thus unaffected by the state of the exciton. In the absence of feedback between the electronic and nuclear degrees of freedom, the composite system cannot properly thermalize. This simply means that excitons will not relax into an equilibrium energetic state, but rather will exhibit behavior associated with the high-temperature limit. Including the effects of excited state forces in our model is straightforward yet very computationally expensive so we omit them.

We justify this omission by recognizing that this approximate method for treating dynamics is accurate in the short time limit. The timescale for energetic relaxation of excitons is expected to be governed by two timescale. First, is the timescale associated with the molecule reorganization time, i.e., the time for excited molecules to relax on the excited state potential energy surface. This timescale is on the order of 100fs, but for delocalized excitons involves relatively small changes in excitation energy. Second, is the timescale associated with exciton migration on a disordered energetic landscape. This timescale is determined by the mobility of excitons and the characteristics of the heterogeneous energetic landscape. In these materials we expect the timescale to be on the order of picoseconds.

---

[1] Ishizaki, A.; Fleming, G. R. *New J. Phys.* **2010**, *12*, 055004.

[2] Shi, L.; Willard, A. P. *J. Chem. Phys.* **2018**, *149*, 094110.